

## Relating estimates of CaCO<sub>3</sub> production, export, and dissolution in the water column to measurements of CaCO<sub>3</sub> rain into sediment traps and dissolution on the sea floor: A revised global carbonate budget

W. M. Berelson,<sup>1</sup> W. M. Balch,<sup>2</sup> R. Najjar,<sup>3</sup> R. A. Feely,<sup>4</sup> C. Sabine,<sup>4</sup> and K. Lee<sup>5</sup>

Received 31 July 2006; revised 15 November 2006; accepted 12 December 2006; published 24 March 2007.

[1] The global CaCO<sub>3</sub> budget is constrained by new estimates of standing stocks, fluxes through the water column, and dissolution in the water column and on the sea floor. Previous estimates of carbonate production and export are indistinguishable within a large range of values, 0.4–1.8 Gt PIC yr<sup>-1</sup>. Globally, excess alkalinity (TA\*) and water mass tracers indicate dissolution of 1.0 Gt PIC yr<sup>-1</sup> between 200 and 1500 m, suggesting production and export must at least equal this amount. Most water column dissolution occurs at high latitudes, and alkalinity fluxes from outer shelf and upper slope sediments (100–1500 m) only support 5–10% of the TA\* inventory. Below 2000 m, the sinking flux of PIC (0.6 Gt PIC yr<sup>-1</sup>) is consistent with the rate of sea floor dissolution (0.4 Gt PIC yr<sup>-1</sup>) plus burial (0.1 Gt PIC yr<sup>-1</sup>). This rain rate constrains the export value to >1.6 Gt PIC yr<sup>-1</sup>. Satellite-based estimates of standing stocks of CaCO<sub>3</sub> indicate a decrease equatorward, which is opposite in trend to sediment trap fluxes. This observation may be explained by an equatorward decrease in sinking particle dissolution, systematic changes in PIC residence time with latitude, or satellite retrieval problems. Globally averaged euphotic zone standing stock (5.4 mmol m<sup>-2</sup>) and export estimates indicate PIC residence times of 5–18 days.

**Citation:** Berelson, W. M., W. M. Balch, R. Najjar, R. A. Feely, C. Sabine, and K. Lee (2007), Relating estimates of CaCO<sub>3</sub> production, export, and dissolution in the water column to measurements of CaCO<sub>3</sub> rain into sediment traps and dissolution on the sea floor: A revised global carbonate budget, *Global Biogeochem. Cycles*, 21, GB1024, doi:10.1029/2006GB002803.

### 1. Introduction

[2] The fate of calcium carbonate produced in the surface ocean is particularly important given the anthropogenic acidification that has occurred over the last century [Kleypas *et al.*, 1999; Caldeira and Wickett, 2003; Feely *et al.*, 2004a; Sabine *et al.*, 2004; Orr *et al.*, 2005; Royal Society, 2005]. Several studies have investigated the response of carbonate-secreting organisms in the face of lowered pH [Gattuso *et al.*, 1998; Kleypas *et al.*, 1999; Langdon *et al.*, 2003; Riebesell *et al.*, 2000; Zondervan *et al.*, 2001; Langdon and Atkinson, 2005] and all indications are that carbonate secretion rates will decline. It is difficult to assess the deleterious effects of acidification on carbonate production because the baseline estimates of how much carbonate is produced and rains through the water column has been shifting. For example, Milliman [1993] estimated carbonate

production in the entire ocean at  $5 \times 10^{13}$  moles CaCO<sub>3</sub> yr<sup>-1</sup> (= 0.6 Gt PIC yr<sup>-1</sup> where PIC is particulate inorganic carbon), which included both neritic and open ocean environments. However, the estimate for open ocean production was based on deep sediment trap data, which provide a lower limit of production. Later, Milliman *et al.* [1999] determined carbonate production in the open ocean at  $6 \times 10^{13}$  moles CaCO<sub>3</sub> yr<sup>-1</sup> (= 0.7 Gt PIC yr<sup>-1</sup>) based on an inventory of alkalinity and the residence time of various water masses. This value was significantly higher than the flux into deep traps and led to the hypothesis that high rates of carbonate dissolution occur within the water column. Balch and Kilpatrick [1996] measured carbonate production in the equatorial Pacific and determined the ratio of PIC to POC (particulate organic carbon) production of ~9%, which, if extrapolated globally would yield an estimate of carbonate production of  $3.5 \times 10^{14}$  moles CaCO<sub>3</sub> yr<sup>-1</sup> (= 4.3 Gt PIC yr<sup>-1</sup>). Recently, Balch *et al.* [2007] reevaluated carbonate production from an assessment of satellite-determined parameters, calcification, and photosynthesis rate determinations, and this value is  $1.3 \times 10^{14}$  moles CaCO<sub>3</sub> yr<sup>-1</sup> (= 1.6 Gt PIC yr<sup>-1</sup>).

[3] If the carbonate system is in steady state, the amount produced in the surface water should equal or exceed the amount falling out of the surface ocean (export), and this would equal the sum of what is remineralized and what is buried. A careful accounting of how much and where

<sup>1</sup>Earth Sciences Department, University of Southern California, Los Angeles, California, USA.

<sup>2</sup>Bigelow Laboratory for Ocean Sciences, West Boothbay Harbor, Maine, USA.

<sup>3</sup>Penn State University, University Park, Pennsylvania, USA.

<sup>4</sup>Pacific Marine Environmental Laboratory, NOAA, Seattle, Washington, USA.

<sup>5</sup>Pohang University of Science and Technology, Pohang, South Korea.

carbonate dissolution occurs is one objective of this study. Recent analyses by *Feely et al.* [2002, 2004a], *Sabine et al.* [2002] and *Chung et al.* [2003] demonstrate the presence of excess alkalinity (TA\*) in water masses at 100–1500 m that they attribute to dissolution occurring during particle sinking. Excess alkalinity is that quantity of alkalinity residing in a water mass following adjustments for the “preformed” alkalinity content and for contributions from AOU [*Feely et al.*, 2002]. TA\* measurements show the highest inputs at depths corresponding to the regional aragonite saturation horizon. Hence one hypothesis was that dissolution of aragonitic particles is responsible for much of the excess alkalinity in the upper 1500 m. However, the high rates of carbonate dissolution in the upper water column are difficult to reconcile using only the export of aragonite, given that there are very few estimates of aragonite production in pelagic waters and this mineral phase is not likely a major component of the total carbonate flux [*Fabry*, 1989]. *Milliman et al.* [1999] considered the enigmatic role of zooplankton guts as a site for carbonate dissolution. However, how much of the TA\* signal can actually be attributed to water column dissolution? *Chen* [2002] has noted the importance of estuarine and coastal benthic processes as a source of alkalinity to upper ocean waters and offers caution to the assumption that all excess alkalinity is attributable to particle dissolution. Also, the models of *Feely et al.* [2002], *Sabine et al.* [2002] and *Chung et al.* [2003] are subject to considerable uncertainties, both with respect to the determination of excess alkalinity and with the assumptions inherent in assigning water mass ages to upper ocean waters. Further, *Friis et al.* [2006, 2007] have shown that mixing of deeper waters with shallower waters may contribute to excess alkalinity in the upper ocean.

[4] Sediment trap data obtained within the last 15 years converge on the value of  $5 \times 10^{13}$  moles  $\text{CaCO}_3 \text{ yr}^{-1}$  (= 0.6 Gt PIC  $\text{yr}^{-1}$ ) falling through the 2000 m depth horizon in the open ocean [*Tsunogai and Noriki*, 1991; *Lampitt and Antia*, 1997; *Francois et al.*, 2002]. If this value is representative of the global ocean, it must constrain both carbonate export and carbonate burial rates. We utilize trap data both as a component in global budgets but also as a means to assess water column dissolution. For example, deep-water masses also contain excess alkalinity [*Feely et al.*, 2002; *Sabine et al.*, 2002; *Chung et al.*, 2003] and modeling TA\* versus water mass age results in an estimate of carbonate dissolution rates in the deep ocean. As with the upper ocean, this approach cannot distinguish water column from benthic processes as the source of excess alkalinity. Sediment trap fluxes at different depths are used to constrain the quantity of carbonate dissolution in the deep sea.

[5] If the amount of carbonate produced and exported from the surface ocean is influenced by ocean acidification [*Orr et al.*, 2005], both the PIC and organic carbon (POC) budgets will be affected (considering the importance of carbonate as a ballast for organic matter export [*Armstrong et al.*, 2002; *Klaas and Archer*, 2002; *Francois et al.*, 2002]). Hence we have revised recent estimates of carbonate production, dissolution and rain into the ocean interior

and focus on examining these fluxes using very different analytical approaches.

## 2. Carbonate Production and Export

[6] We distinguish between carbonate production and export, although the literature can be confusing regarding the difference. Here we define carbonate production as the vertically integrated calcification rate in the surface (i.e., euphotic) layer, whereas carbonate export is the sinking flux out of the surface layer. The two differ because of dissolution of  $\text{CaCO}_3$  within the surface layer and departure from steady state. *Balch et al.* [2007] summarized calcification rate measurements (= carbonate production) at six open ocean sites and show that carbonate production averages  $\sim 3\%$  of organic carbon primary production. By refining this estimate with satellite data of temperature, chlorophyll, PIC standing stock and known parameters such as day length and depth of mixed layer, they were able to estimate global carbonate production in 2002 at  $1.6 \pm 0.3$  Gt PIC  $\text{yr}^{-1}$ . *Poulton et al.* [2006] present PIC production data for the Atlantic, which extrapolated globally yields a value of 3 Gt PIC  $\text{yr}^{-1}$ . The only other estimates of global carbonate production that we are aware of are from *Moore et al.* [2002, 2004], who embedded a detailed food web model with explicit representation of carbonate producers into global physical models. The first of the two studies utilized a 1-D mixed layer model applied globally, whereas the second used the 3-D circulation field from an ocean general circulation model. These studies estimate global carbonate production as 1.1 and 0.5 Gt PIC  $\text{yr}^{-1}$ , respectively.

[7] There are many more estimates of global carbonate export from the euphotic zone, many of which rely, in one way or another, on the alkalinity distribution. A range of 0.6 to 1.5 Gt PIC  $\text{yr}^{-1}$  is derived from studies that have utilized simple circulation models (box or 1-D): 0.6 and 1.5 Gt PIC  $\text{yr}^{-1}$  from two different versions of the 12-box model of *Garcon and Minster* [1988]; 0.9 Gt PIC  $\text{yr}^{-1}$  from a combination 1-D/box model of *Shaffer* [1993]; and 1.4 Gt PIC  $\text{yr}^{-1}$  for the 3-stacked-box model of *Chuck et al.* [2005]. A range of 0.6 to 1.8 is found from three-dimensional circulation models with simplified carbonate cycle parameterizations, which are typically tuned to reproduce the observed alkalinity distribution: 0.7 Gt PIC  $\text{yr}^{-1}$  from *Bacastow and Maier-Reimer* [1990]; 0.6–0.8 Gt PIC  $\text{yr}^{-1}$  from *Yamanaka and Tajika* [1996]; 1.65 Gt PIC  $\text{yr}^{-1}$  from *Archer et al.* [1998]; and 1.8 Gt PIC  $\text{yr}^{-1}$  from *Murnane et al.* [1999]. The mechanistic models of *Moore et al.* [2002, 2004], which were not evaluated with alkalinity measurements, estimate carbonate export of 0.5 and 0.4 Gt PIC  $\text{yr}^{-1}$ , respectively.

[8] Carbonate export has been estimated in two additional ways: seasonal alkalinity drawdowns and estimates of the molar rain ratio ( $\text{CaCO}_3$  to organic C) of export in combination with estimates of organic carbon export. The former, made by *Lee* [2001], yields  $1.4 \pm 0.3$  Gt PIC  $\text{yr}^{-1}$ , which could be construed as a lower limit because it probably underestimates export in regions like the equatorial Pacific, which sustain substantial export without generating seasonal variations in alkalinity. The latter approach was used by

**Table 1.** Summary of CaCO<sub>3</sub> Dissolution Flux Estimates in the Upper Ocean<sup>a</sup>

Location	Area, $\times 10^{12}$ m <sup>2</sup>	mmol m <sup>-2</sup> day <sup>-1</sup>	Gt PIC yr <sup>-1</sup>
Atlantic			
>40°N	12.4	1.7	0.06
40°N–40°S	49.1	0.1	0.01
>40°S	18.5	0.6	0.04
Indian			
40°N–40°S	42.8	0.9	0.16
>40°S	27.1	1.2	0.14
Pacific			
>40°N	9.4	1.7	0.07
40°N–5°N	54.5	1.4	0.33
5°N–5°S	11.3	0.4	0.02
5°S–40°S	40.6	0.0	0.00
>40°S	36.3	1.0	0.16
Total			1.0

<sup>a</sup>These values have been determined from TA\* and water mass CFC age models for regions in the Atlantic, Indian, and Pacific oceans and for depths between 200 and 1500 m. The uncertainty in these rates is approximately 50%.

*Sarmiento et al.* [2002], who estimated the global mean rain ratio to be 0.053 (based on vertical alkalinity and nitrate gradients) and combined this with the *Laws et al.* [2000] estimate of export production (11 Gt POC yr<sup>-1</sup>) to arrive at global carbonate export of 0.6 Gt PIC yr<sup>-1</sup>.

[9] In theory, sediment traps located in the upper 200 m of the water column should constrain export flux. However, traps located at shallow depths are subject to hydrodynamic and biological artifacts that may bias the collection of settling particles. It is not certain whether this bias would generate high or low carbonate flux values, however. Floating traps deployed in the Pacific Ocean at low latitudes [*Rodier and Le Borgne*, 1997] yield CaCO<sub>3</sub> fluxes of 0.9–3.0 mmol PIC m<sup>-2</sup> d<sup>-1</sup> falling into traps at 125–150 m. Floating traps in the NE Pacific [*Wong et al.*, 1999] yield fluxes of 2.7 mmol m<sup>-2</sup> d<sup>-1</sup> falling through the 50 m horizon. If these regional measurements were extrapolated globally, the fluxes translate into export rates of 1.4 to 4.7 Gt PIC yr<sup>-1</sup> (given ocean area of  $3.6 \times 10^{14}$  m<sup>2</sup>). The relative importance of autotrophs versus heterotrophs in PIC export is not well established, but an estimate by *Schiebel* [2002] constrains foraminiferal flux at 0.1–0.2 mmol m<sup>-2</sup> d<sup>-1</sup> or 0.2–0.3 Gt PIC yr<sup>-1</sup>. This term in the carbonate production and export budgets may be overlooked using modeling and satellite approaches. Floating traps integrate fluxes over a short time period, and are subject to high temporal variability; the floating trap fluxes reported here are higher than the other estimates of export and this may be related to the limited size of the data set and the difficulties in interpreting shallow trap data. Novel sediment trap designs (*K. O. Buesseler et al.*, Estimating upper ocean particle fluxes with sediment traps, submitted to *Journal of Marine Research*, 2007) will, hopefully, improve this situation.

[10] In summary, estimates of global carbonate production are between 0.5 and 1.6 Gt PIC yr<sup>-1</sup>, whereas those for global carbonate export are between 0.4 and 1.8 Gt PIC yr<sup>-1</sup> (not including floating trap data). These fluxes are indistin-

guishable, though, in principle, export should be less than or equal to production. Although we cannot reliably estimate, on global scales, the amount of CaCO<sub>3</sub> dissolution occurring in the euphotic zone, we note in the *Moore et al.* [2002, 2004] models, the fraction of carbonate production that is exported is 50% and 70%, respectively. This contrasts sharply with that of organic matter cycling. Recent global estimates of organic matter export are between 10 and 15 Gt POC yr<sup>-1</sup> [*Jin et al.*, 2007], whereas global primary production estimates are in the range of 40–50 Gt POC yr<sup>-1</sup>; that is, approximately 20–40% of global primary production is exported. Trap, benthic data, and new models (presented in the following sections) help constrain production and export fluxes at values >1.6 Gt PIC yr<sup>-1</sup>.

### 3. Dissolution in the Upper Water Column

[11] Profiles of carbonate dissolution in the water column of the upper ocean [*Feely et al.*, 2004a] indicate maximum dissolution occurs between 250 and 750 m although in the Atlantic Ocean, dissolution occurs through 2000 m. The approach used by these authors provide estimates of alkalinity increase per mass of water per time ( $\mu$ equivalents TA\* kg<sup>-1</sup> yr<sup>-1</sup>) that were converted to units of carbonate dissolution given that one mole of carbonate dissolved produces two equivalents of excess alkalinity. By making this conversion, the assumption was that the only source of TA\* was carbonate dissolution. Here we re-analyzed those rates by dividing the Atlantic, Indian and Pacific Oceans into latitudinal regions. For each region, the water mass age, which was based on the most recent CFC age models and data available, and its TA\* value was determined for depths >200 m and <1500 m. We also make the assumption that the source of alkalinity is carbonate dissolution and use the area and volume of each region to convert dissolution rates of  $\mu$ moles PIC kg<sup>-1</sup> yr<sup>-1</sup> to Gt PIC yr<sup>-1</sup> and mmol PIC m<sup>-2</sup> yr<sup>-1</sup> (Table 1).

[12] The relationship between excess alkalinity and water mass age does not indicate where that signal was derived, although the assumption was that carbonate particles dissolve while settling. Another interpretation is that sedimentary processes contribute excess alkalinity to the water column of the upper ocean. In the upper water column, contact between the ocean and sediments occurs at the edges of the basin. If excess alkalinity were entering the ocean horizontally from the continental margins, one would expect to see onshore/offshore gradients in the TA\* distribution, if mixing is not sufficiently fast to homogenize this parameter. While these gradients are not observed in E-W transects across the Pacific [*Feely et al.*, 2002], it is apparent from Table 1 that the northern and southern regions of the ocean basins have higher carbonate dissolution rates per unit area, than the central portions. The highest rates of excess alkalinity accumulation are in the North Pacific and North Atlantic Ocean basins.

[13] To assess the role of sediment processes to the TA\* burden in the upper water column, we summarized benthic chamber alkalinity flux measurements made along the California margin including sites on the outer shelf and upper slope [*Berelson et al.*, 1996; *Reimers et al.*, 1992]

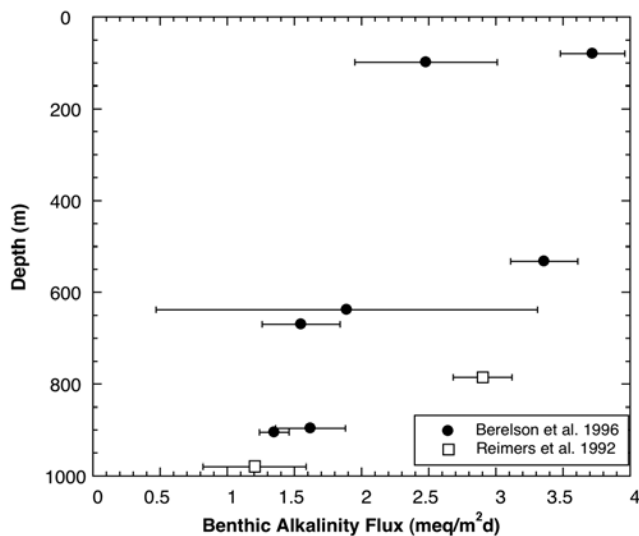


**Figure 1.** Total alkalinity fluxes from sediments located off the Central California Margin. Error bars represent the s.d. of the measurement.

(Figure 1). Between 100 and 800 m the average alkalinity flux is  $\sim 2.5 \text{ meq m}^{-2}\text{d}^{-1}$ , this is very close to the rate at which excess alkalinity is added to the water column of the N. Pacific ( $3.4 \text{ meq m}^{-2}\text{d}^{-1}$  from Table 1). Water that comes in contact with outer shelf sediments ( $\sim 100 \text{ m}$ ) may mix with deeper waters or get subducted to greater depths, hence these sediments may contribute to  $\text{TA}^*$  at depths  $>200 \text{ m}$ .

[14] The alkalinity flux from these margins sediments is attributable to both carbonate dissolution and sulfate reduction whereby the sulfide reacts with iron oxyhydroxides producing alkalinity [Hammond *et al.*, 1999]. Relating the flux of alkalinity from sediments to the injection of alkalinity per unit area of water requires a comparison between the areal extent of the water column signal to the area of the sediment source. We utilized a 2-min gridded global relief map (ETOPO2V2—NOAA) to assess the hypsometric distribution of North Pacific Ocean sea floor area and determined that approximately 8% of the area of the N. Pacific (between the equator and Aleutian chain) lies between 100–1500 m water depth (including the Sea of Okhotsk and the China Sea in this calculation). Thus, although benthic alkalinity fluxes per unit area of sea floor are comparable to the water column integrated flux from  $\text{TA}^*$  calculations, the area of shelf and slope sediments (100–1500 m) in the North Pacific is too small to contribute more than 5–8% to the water column excess alkalinity standing stock.

[15] As a further check of this conclusion, we considered that the alkalinity flux from California margin sediments are different than fluxes from other North Pacific margins. Berelson *et al.* [1996] noted that  $\text{TCO}_2$  (total  $\text{CO}_2$ ) fluxes are comparable between the Washington shelf [Devol and Christensen, 1993], Alaskan shelf [Grebmeier and McRoy, 1989] and California shelf [Berelson *et al.*, 2003], all averaging  $15 \text{ mmol m}^{-2}\text{d}^{-1}$ . Previous work has shown that

$\text{TCO}_2$  fluxes correlate positively with alkalinity fluxes (Figure 2). Assuming other margins show a decrease in  $\text{TCO}_2$  flux with depth comparable to the pattern displayed off the California margin [Berelson *et al.*, 1996], and using the relationship between  $\text{TCO}_2$  and alkalinity fluxes (Figure 2), the average alkalinity flux from sediments between 100 and 1500 m around the northeastern Pacific margin is not more than  $3.5 \text{ meq m}^{-2}\text{d}^{-1}$ . Thus the consideration of other regions around the North Pacific margin does not change our conclusion that sediments between 100–1500 m are not likely a major source of  $\text{TA}^*$  to the water column. However, the alkalinity flux from sediments at water depths  $<100 \text{ m}$  may be an additional source of  $\text{TA}^*$ , and these waters must be considered in a final assessment.

[16] The rate of  $\text{TA}^*$  addition to the upper water column (Table 1) implies that the amount of carbonate falling through this water column decreases by  $1.7 \text{ mmol m}^{-2}\text{d}^{-1}$  between export and  $\sim 1500 \text{ m}$ , throughout the North Pacific at latitudes  $>40^\circ\text{N}$ . If this process is occurring, sediment traps should detect a change in carbonate flux of this amount. A summary of five years of data from the N. E. Pacific Station P [Wong *et al.*, 1999] includes carbonate fluxes at 200 and 1000 m. The difference in mean carbonate flux between these traps is  $0.23 \text{ mmol m}^{-2}\text{d}^{-1}$ , indicating dissolution of particles between these depths, but not enough to support the value derived from  $\text{TA}^*$  analysis. It is possible that the shallow trap undercollected and/or the deeper trap overcollected or that Station P is not representative of other portions of the North Pacific. Wong *et al.* [1999] also report carbonate fluxes into floating sediment traps deployed at a depth of 50 m. The mean carbonate flux at 50 m was  $2.7 \text{ mmol m}^{-2}\text{d}^{-1}$  and the average flux into

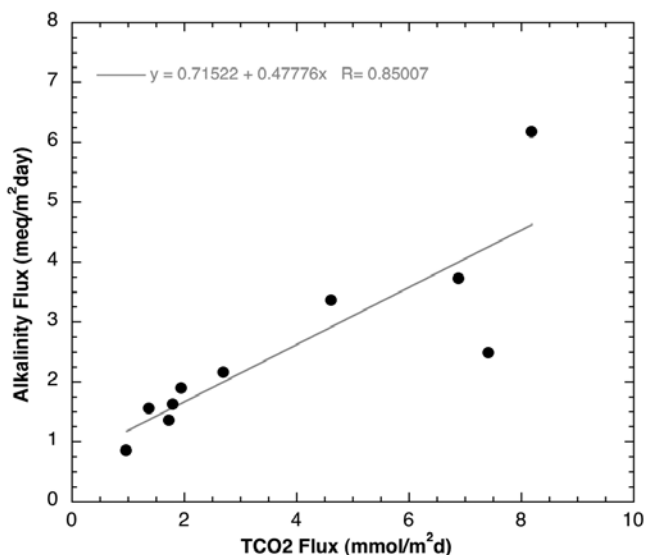
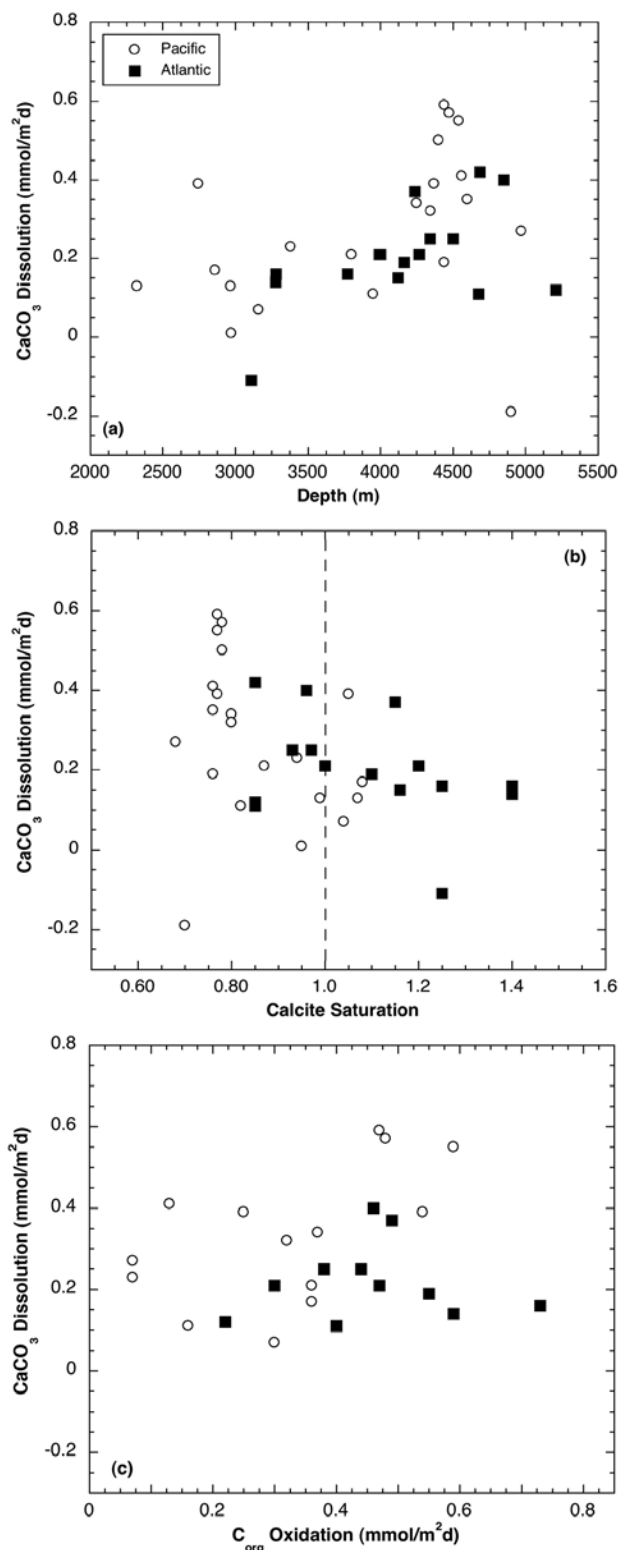


**Figure 2.** Relationship between  $\text{TCO}_2$  and total alkalinity fluxes as derived from benthic chamber experiments conducted on the Central and Southern California Margin [Berelson *et al.*, 1996]. Linear regression indicates the correlation between these parameters and thus how well  $\text{TCO}_2$  fluxes can be used to predict alkalinity fluxes.



traps at 1000 m was  $0.6 \text{ mmol m}^{-2}\text{d}^{-1}$ . Thus, if the floating trap flux value is representative of  $\text{CaCO}_3$  export, there may be sufficient carbonate material raining from the surface ocean to support a water column dissolution rate of  $1.7 \text{ mmol m}^{-2}\text{d}^{-1}$ . However, the large uncertainties in floating and shallow sediment trap flux data requires caution when they are used to evaluate flux budgets [Buesseler, 1991; Yu *et al.*, 2001].

[17] From a global budget perspective, we can compare the range of export estimates,  $0.4\text{--}1.8 \text{ Gt PIC yr}^{-1}$ , with the integrated (200–1500 m) dissolution rates of Table 1 ( $1.0 \text{ Gt PIC yr}^{-1}$ ). This comparison suggests that the export estimates of  $<1.0 \text{ Gt PIC yr}^{-1}$  are low. However, there may be uncertainties in all of these estimates of  $\pm 50\%$ . While Friis *et al.* [2006, 2007] recently suggested that a significant fraction of the  $\text{TA}^*$  inventory in the main thermocline may be derived from deeper water via transport and boundary mixing, and that this process may inflate dissolution rate estimates, we also note that export fluxes based on floating traps are large enough to account for shallow dissolution occurring at a rate of  $1.0 \text{ Gt PIC yr}^{-1}$  and still allow for the flux of carbonate to the deep ocean.

#### 4. Dissolution in the Deep Ocean and on the Deep Sea Floor

[18] Excess alkalinity and water mass ages determined using  $^{14}\text{C}$  tracer data were used to define carbonate dissolution rates in the deep waters of the Pacific [Feely *et al.*, 2002], Indian [Sabine *et al.*, 2002] and Atlantic Oceans [Chung *et al.*, 2003]. These rates are an order of magnitude less than in the upper water column: deep rates average  $0.05$ ,  $0.06$  and  $0.05 \mu\text{moles CaCO}_3 \text{ kg}^{-1} \text{ yr}^{-1}$  for the Pacific, Indian and Atlantic, respectively. These rates are defined from water masses deeper than 1500 m and yet it is not clear whether the addition of alkalinity occurs continuously from 1500 m to the sea floor or at particular horizons. As there is less  $\text{TA}^*$  data for the deep ocean, this parameter had to be averaged over larger depth and space domains than the shallow water estimates.

[19] Profiles of excess alkalinity generally increase toward the sediment implying that much of the alkalinity is coming from dissolution at or near the sea floor. This is most apparent in profiles from the Arabian Sea and the Bay of Bengal [Sabine *et al.*, 2002] but is also detected in the Atlantic and Pacific basins. However, there also appears to be maxima in dissolution that correspond with the depth of the calcite saturation horizon. Again, an increase in  $\text{TA}^*$  with depth does not define whether particles dissolve during settling or if dissolution is occurring on the sea floor.

[20] The deep ocean is in contact with sea floor sediments, thus a sedimentary source of  $\text{TA}^*$  might be detected

**Figure 3.** (a) Compilation of sediment carbonate dissolution rate determinations from Atlantic and Pacific Ocean sites (Table 2). (b) Dissolution rates as a function of calcite saturation state ( $\omega$ ).  $\omega$  was determined following the procedures described by Sabine *et al.* [2002]. (c) Dissolution rates as a function of organic carbon oxidation ( $\text{C}_{\text{ox}}$ ).

**Table 2.** Benthic Carbonate Dissolution Rate Measurements Made Using In Situ Sample Collection Methods<sup>a</sup>

Site/Reference	Latitude	Longitude	Depth, m	Omega (Calcite)	CaCO <sub>3</sub> , mmol/m <sup>2</sup> day	C <sub>ox</sub> , mmol/m <sup>2</sup> day
<i>Pacific/Abysal</i>						
Ontong Java						
H(96)pH	00°00'S	159°40'E	2322	1.07	0.13 ± 0.03	...
	00°00'S	160°25'E	2966	0.99	0.13 ± 0.03	...
J(94)I	00°00'S	160°25'E	2972	0.95	0.01 ± 0.12	...
	00°00'S	162°41'E	4439	0.76	0.19 ± 0.05	...
EQPAC						
B(94)I	01°00'N	102°48'W	3380	0.94	0.23 ± 0.11	0.07 ± 0.46
	00°00'N	110°30'W	3800	0.87	0.21 ± 0.08	0.36 ± 0.25
	00°00'N	121°36'W	4250	0.80	0.34 ± 0.07	0.37 ± 0.16
	00°00'N	139°54'W	4370	0.77	0.39 ± 0.12	0.25 ± 0.15
	01°50'S	139°42'W	4475	0.78	0.57 ± 0.05	0.48 ± 0.11
	00°00'N	139°48'W	4440	0.77	0.59 ± 0.05	0.47 ± 0.09
	02°02'N	140°12'W	4540	0.77	0.55 ± 0.07	0.59 ± 0.12
	05°05'N	139°42'W	4560	0.76	0.41 ± 0.04	0.13 ± 0.08
B(90)I	11°00'N	140°00'W	4900	0.70	-0.19 ± 0.13	...
	01°00'N	139°00'W	4400	0.78	0.50 ± 0.10	...
	05°00'N	138°00'W	4600	0.76	0.35 ± 0.13	...
Southern Ocean						
S(01)pw	66°08'S	169°37'W	3160	0.99	0.07 ± 0.02	0.30
	64°12'S	170°07'W	2745	1.05	0.39 ± 0.12	0.54
	63°10'S	169°51'W	2860	1.08	0.17 ± 0.03	0.36
	60°15'S	170°11'W	3950	0.82	0.11 ± 0.01	0.16
	58°41'S	169°59'W	4345	0.80	0.32	0.32
	56°53'S	170°10'W	4970	0.68	0.27	0.07
<i>Pacific/Margin</i>						
Central California						
J(97)I <sup>b</sup>	35°38'N	121°37'W	790	0.90	0.90 ± 0.49	2.0
	35°37'N	121°50'W	1010	0.93	0.96 ± 0.98	1.8
	36°06'N	122°36'W	3340	0.83	2.90 ± 1.81	2.0
	35°27'N	122°21'W	3745	0.83	1.04 ± 1.12	1.8
R(92)pw/I	35°27'N	122°21'W	4075	0.81	0.90	1.0
B(96)I	35°24'N	121°06'W	231	2.06	2.2 ± 1.0	6.0 ± 1.5
	35°42'N	121°30'W	532	1.10	0.8 ± 0.6	3.8 ± 2.9
	35°12'N	121°18'W	638	1.00	0.2 ± 0.7	1.8 ± 1.8
	35°12'N	121°19'W	670	0.92	0.3 ± 0.2	1.1 ± 0.3
	35°30'N	121°36'W	1010	0.93	0.1 ± 0.3	0.9 ± 0.8
	36°12'N	122°24'W	1358	0.97	0.6 ± 0.2	1.8 ± 0.6
	36°06'N	122°24'W	2025	0.94	0.4 ± 0.1	1.1 ± 0.3
	36°07'N	122°18'W	3375	0.83	0.4 ± 0.1	0.7 ± 0.3
Southern California						
B(96)I	33°30'N	118°24'W	896	0.86	0.0 ± 0.2	1.8 ± 0.4
	33°42'N	118°48'W	905	0.86	0.0 ± 0.2	1.7 ± 0.4
	33°18'N	118°36'W	1300	0.86	0.1 ± 0.3	1.2 ± 0.9
	33°00'N	119°42'W	1514	0.86	0.6 ± 0.3	0.9 ± 0.6
	32°36'N	118°06'W	2053	0.91	0.4 ± 0.2	1.1 ± 0.3
	32°24'N	120°36'W	3707	0.78	0.2 ± 0.1	0.4 ± 0.1
B(87)I	33°30'N	118°24'W	900	0.86	0.27	1.6 ± 0.6
	32°57'N	119°00'W	1800	0.89	0.59	1.3 ± 0.2
J(90)I	33°42'N	118°48'W	905	0.85	0.0	2.7
<i>Atlantic/Abysal</i>						
Cape Verde Rise						
J(94)I	18°28'N	21°02'W	3110	1.25	-0.11 ± 0.60	...
Sargasso						
H(94)pH <sup>c</sup>	36°16'N	71°31'W	4236	1.15	0.37 ± 0.10	0.49 ± 0.08
	34°33'N	71°35'W	4501	1.02	0.25 ± 0.08	0.38 ± 0.05
	34°20'N	70°21'W	5210	0.85	0.12 ± 0.04	0.22 ± 0.03
Ceara Rise						
M(96)pw <sup>d</sup>	5°16'N	44°09'W	3279	1.40	0.14	0.59
H(97)pH	5°16'N	44°09'W	3280	1.40	0.16	...
M(96)pw <sup>d</sup>	5°27'N	44°01'W	3772	1.25	0.16	0.73
	5°17'N	43°34'W	3990	1.20	0.21 ± 0.10	0.47
H(97)pH	5°17'N	43°34'W	4000	1.20	0.21	...
	5°30'N	43°30'W	4120	1.16	0.15	...
M(96)pw <sup>d</sup>	5°33'N	43°36'W	4164	1.10	0.19	0.55
	5°46'N	43°38'W	4267	1.00	0.21	0.30
	5°45'N	43°24'W	4342	0.93	0.25	0.44
	6°10'N	42°53'W	4675	0.85	0.11	0.40
H(97)pH	6°10'N	42°53'W	4685	0.85	0.42	...

**Table 2.** (continued)

Site/Reference	Latitude	Longitude	Depth, m	Omega (Calcite)	CaCO <sub>3</sub> , mmol/m <sup>2</sup> day	C <sub>ox</sub> , mmol/m <sup>2</sup> day
PAP						
R(01) <sup>e</sup>	48°50'N	16°30'W	4850	0.96	0.4 ± 0.1	0.46 ± 0.37
<i>Atlantic/Margin</i>						
New England						
H(94)pH	39°37'N	69°40'W	2159	1.75	0.51 ± 0.15	0.82 ± 0.14
Cape Hatteras						
J(00) <sup>f</sup>	36°05'N	74°44'W	850	3.53	0.71 ± 0.29	3.27
	36°30'N	74°41'W	740	3.53	4.34 ± 0.74	6.16
	32°42'N	75°51'W	2927	1.48	1.41 ± 0.42	0.97
	37°20'N	74°44'W	761	3.53	1.72 ± 0.55	3.37
	36°27'N	74°43'W	755	3.53	4.76 ± 0.51	7.23
	35°23'N	74°50'W	855	2.90	2.00 ± 0.93	6.18
	36°09'N	74°03'W	2635	1.60	1.66 ± 0.67	2.58
	36°20'N	74°44'W	721	3.53	5.09 ± 0.94	2.66
	36°20'N	74°44'W	730	3.53	8.31 ± 0.14	6.89
	35°51'N	74°49'W	607	4.65	6.00 ± 1.99	8.23
Gabon						
P(03)pH/pw	00°41'S	08°23'E	1251	1.80	0.99	1.1
W(01)	00°41'S	08°23'E	1251	1.80	0.55	0.53
	02°04'S	08°38'E	1317	1.65	0.58	0.97

<sup>a</sup>Abbreviations: l, lander; pH, microelectrode; pw, pore water; B(87), Berelson et al. [1987]; B(90), Berelson et al. [1990]; B(94), Berelson et al. [1994]; H(94), Hales et al. [1994]; H(96), Hales and Emerson [1996]; H(97), Hales and Emerson [1997]; J(90), Jahnke [1990]; J(94), Jahnke et al. [1994]; J(97), Jahnke et al. [1997]; J(00), Jahnke and Jahnke [2000]; M(96), Martin and Sayles [1996]; P(03), Pfeifer et al. [2003]; R(92), Reimers et al. [1992]; R(01), Rabouille et al. [2001]; S(01), Sayles et al. [2001]; W(01), Wenzhofer et al. [2001]; Omega refers to the saturation state of calcite at or near the location cited, and C<sub>ox</sub> is the rate of organic carbon oxidation in the sediment.

<sup>b</sup>Uses calcium flux values and C<sub>ox</sub> from R(92).

<sup>c</sup>Uncertainty represents the range of values.

<sup>d</sup>Pore water measured values reported, if two values are given the average is reported.

<sup>e</sup>C<sub>ox</sub> from Ståhl et al. [2004].

<sup>f</sup>Uses calcium flux values and averages stations J&K and L&M.

depending on the strength of vertical mixing. We have assembled a compilation of all in situ benthic dissolution rate data (Table 2), which indicates that sedimentary dissolution fluxes increase with depth to approximately 4500 m, then decrease (Figure 3). The decline in dissolution rate at depths >4500 m is likely related to the paucity of carbonate within the sediments at the sites where measurements were made. The distribution of in situ dissolution measurements is meager; thus patterns in this pooled data should not be overinterpreted. Note that no dissolution rate measurements are reported for the Indian Ocean. The summary provided in Table 2 includes values of calcite saturation state at or near the location of benthic dissolution measurements. It appears that benthic dissolution rates in the deep ocean are weakly related to calcite saturation state and poorly correlated with the amount of organic carbon oxidized on the sea floor (Figure 3).

[21] From a modeling approach, Archer [1996] predicted that benthic dissolution rates on the deep sea floor would range from 0.2–0.3 mmol CaCO<sub>3</sub> m<sup>-2</sup>d<sup>-1</sup>. We find the average of all benthic dissolution rate measurements for sites below 2000 m is 0.24 ± 0.17 mmol CaCO<sub>3</sub> m<sup>-2</sup>d<sup>-1</sup>, where the uncertainty represents the standard deviation of 37 measurements. The average benthic dissolution rate in the deep Pacific Ocean is 0.27 ± 0.20 mmol CaCO<sub>3</sub> m<sup>-2</sup>d<sup>-1</sup> and 0.20 ± 0.13 in the Atlantic. Although the Pacific has deep water that is more undersaturated with respect to calcite than does the Atlantic, the comparison of dissolution rates was made over similar depth ranges and at sites where the organic carbon rain rates were comparable (Figure 3). Feely et al. [2004a] reported that the Pacific and Atlantic

Ocean deep water mass-derived dissolution rates are similar, 0.05 μmoles CaCO<sub>3</sub> kg<sup>-1</sup> yr<sup>-1</sup>. Within uncertainties, the rate of TA\* addition to the deep Atlantic is equal to that of the deep Pacific and the measured rates of benthic dissolution are also equal. If we assume that deep water masses are 1500–2000 m thick, the tracer-derived dissolution rate of 0.05 μmoles CaCO<sub>3</sub> kg<sup>-1</sup> yr<sup>-1</sup> translates into a dissolution flux of 0.21–0.28 mmol CaCO<sub>3</sub> m<sup>-2</sup>d<sup>-1</sup> which is similar to the measured values. The excess alkalinity signal in deep water could be supplied by benthic dissolution if the water masses are in continuous contact with the sea floor, which is a reasonable assumption for the deep ocean. Although carbonate dissolution occurs in sediments at all depths, the depth range where dissolution rates are significantly greater than 0 is from approximately 3000–5000 m (Figure 3a).

[22] The preceding discussion suggests that nearly all TA\* added to bottom water could be derived from the sea floor, yet sediment trap data indicates that there is some dissolution of carbonate particles as they settle between 2000 and 4500 m. However, this rate is generally small, <0.05 mmol m<sup>-2</sup>d<sup>-1</sup> [Feely et al., 2004a], which is much lower than the average in situ benthic dissolution rate. We conclude that particle settling is a minor source of the TA\* in deep water: approximately 80–90% of the excess alkalinity signal in deep water can be supplied by benthic dissolution.

[23] If accurate and representative, sediment traps constrain both the flux of PIC rain into the deep ocean and the export flux. The compilation of sediment trap flux data of Francois et al. [2002] includes a survey of trap data for depths >2000 m from the Atlantic, Pacific and Indian

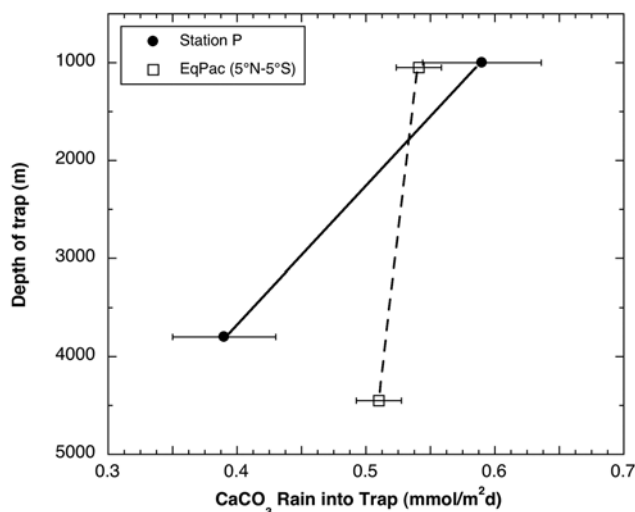


**Figure 4.** Average rain of  $\text{CaCO}_3$  into sediment traps located near 1000 and 4000 m. The Station P trap data is presented by Wong *et al.* [1999] and the EqPac data is a compilation of traps located between  $5^\circ\text{N}$  and  $5^\circ\text{S}$  and represents an average of fluxes reported by Dymond and Collier [1988] and Honjo *et al.* [1995] summarized by Berelson *et al.* [1997]. Although there is seasonal, annual and spatial variability in fluxes, the error bars represent the standard error of the mean for  $n$  annual average flux values. At EqPac,  $n = 8$ , at Station P,  $n = 5$  at 1000 m and  $n = 9$  at 3800 m.

Oceans. The average flux of carbonate to traps in the Atlantic and Pacific Oceans (where benthic dissolution rate measurements have been made) is  $0.32 \pm 0.22 \text{ mmol CaCO}_3 \text{ m}^{-2} \text{ d}^{-1}$ . This includes 51 measurements made primarily in the Northern Hemisphere. If the Indian Ocean trap data are included, the global average increases to  $0.38 \text{ mmol m}^{-2} \text{ d}^{-1}$ . Given the carbonate rain to depths below 2000 m in the Atlantic and Pacific is  $0.32 \text{ mmol m}^{-2} \text{ d}^{-1}$  and the average of benthic dissolution measurements is  $0.24 \text{ mmol m}^{-2} \text{ d}^{-1}$ , this difference allows for a small quantity of carbonate arriving on the sea floor which does not dissolve. A summary of Holocene sediment mass accumulation rates by Catubig *et al.* [1998] provides an estimate of carbonate accumulation in the deep sea,  $0.08 \text{ mmol m}^{-2} \text{ d}^{-1}$ . Although there is considerable uncertainty in all these global flux estimates, there is a remarkable consistency between these three data sets: rain = benthic dissolution + burial. The uncertainty in this balance leaves room for some PIC dissolution during settling through the deep-water column, however, the predominance of evidence suggests that most deep-water excess alkalinity is derived from benthic dissolution.

## 5. Water Column Chemistry and Carbonate Rain Rates: Regional Budgets

[24] The global averages presented above are likely to obscure regional patterns that may point to changes in carbonate cycling occurring on the anthropogenic timescale. For example, the summary of carbonate rain, dissolution

and burial at the Porcupine Abyssal Plain station [Rabouille *et al.*, 2001] and at US-JGOFS EqPac sites [Berelson *et al.*, 1997] both suggest that carbonate budgets are not completely balanced. Whereas the results of Berelson *et al.* [1997] were interpreted as a change in benthic dissolution rates that may have occurred  $\sim 3000$  years ago, Rabouille *et al.* [2001] contend that recent changes in surface ocean ecology have decreased the flux of PIC to the deep North Atlantic within the last 20–100 years. They found insufficient input of PIC to balance dissolution and burial rates. A connection between this observation and the invasion of anthropogenic  $\text{CO}_2$  and acidification of the North Atlantic [Sabine *et al.*, 2004] is conjecture, yet speaks to the importance of assessing regional carbonate budgets.

[25] There is a large change in the depth of the calcite saturation horizon occurring around  $20^\circ\text{N}$ – $30^\circ\text{N}$  in the North Pacific Ocean [Feely *et al.*, 2004a]. The horizon shoals from about 2700 m at the equator to  $<1000$  m north of  $30^\circ$  within the central Pacific basin. Sediment traps located at Ocean Station P ( $50^\circ\text{N}$ ,  $145^\circ\text{W}$  [Wong *et al.*, 1999]) and in the equatorial Pacific ( $140^\circ\text{W}$  [Honjo *et al.*, 1995]) provide an opportunity to investigate the impact of water column dissolution (Figure 4). As stated earlier, traps at depths shallower than 1000 m, especially where current flow may be vigorous, are likely to overcollect or undercollect material; hence their flux values are less accurate. However, multiple years of collection, as available at EqPac and Station P, may help minimize random uncertainties. Systematic trapping uncertainties may still skew the data. The pattern of carbonate rain versus trap depth does show that there is likely more particle dissolution occurring in the 1000–4000 m depth range in the North Pacific than in the equatorial Pacific. Given the severe shoaling of the calcite saturation horizon in the North Pacific, this is exactly what thermodynamic control on carbonate dissolution would predict. Moreover, this trend implies that acidification of the water column will likely decrease the flux of carbonate due to water column dissolution. Although the magnitude of water column dissolution in deep water is small compared to the rate at which benthic dissolution is occurring, dissolution of settling carbonate particles is happening and occurs more in high latitudes, where the saturation horizon is relatively shallow, than in low latitudes. We suggest that dissolution of settling particles occurs both in the upper water column and deep water column, to a greater extent in the upper water column, and to a greater extent at high latitudes compared to low latitudes.

## 6. PIC:POC

[26] Satellite imagery has been used to determine the standing stock of PIC and POC in global waters [Balch *et al.*, 2005], yet one outstanding question is whether the carbonate that a satellite detects includes most of the carbonate that sinks to the ocean interior. The following calculations and summaries shed some light on this question.

[27] By integrating the data of Balch *et al.* [2005], we determined the global average standing stock of PIC in the euphotic zone,  $5.4 \text{ mmol m}^{-2}$  (excluding  $>80^\circ$  latitudes).

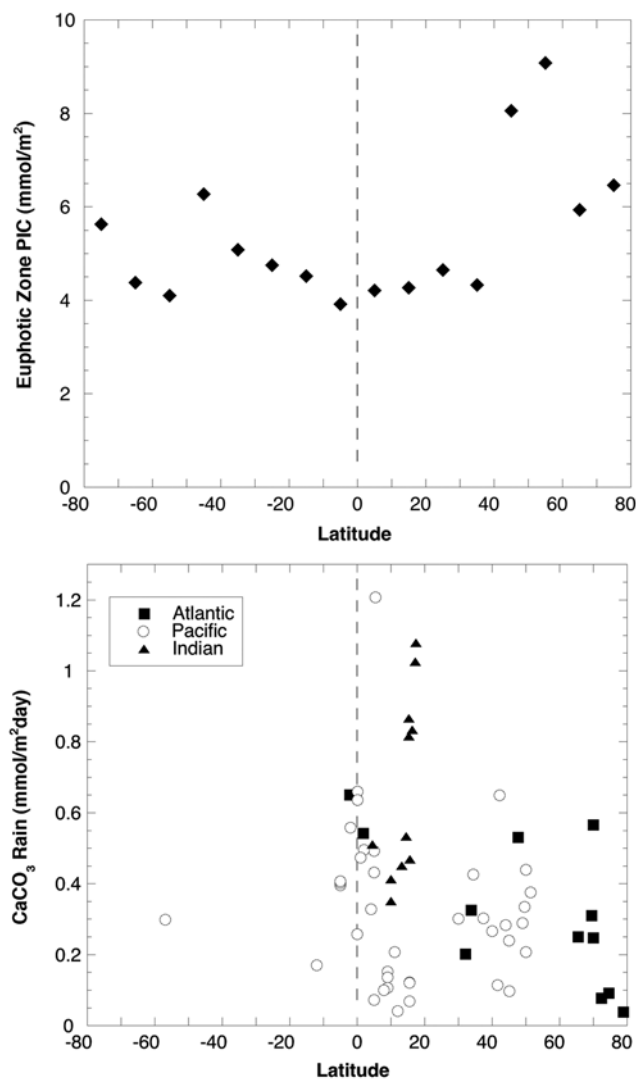


**Figure 5.** (top) Annual average of PIC standing stock in the euphotic zone of the global ocean (derived from *Balch et al.* [2005]). (bottom) Sediment trap flux compilation from *Francois et al.* [2002]. Each point represents the results from a single trap located between 2000 and 5200 m.

Given the range of PIC export,  $0.4\text{--}1.8\text{ Gt PIC yr}^{-1}$  ( $= 0.3\text{--}1.1\text{ mmol m}^{-2}\text{d}^{-1}$ ), the carbonate particles seen by satellite imagery reside in the surface ocean for a period of 5–18 days. *Balch and Kilpatrick* [1996] made measurements of PIC standing stocks and the rate of calcification along a transect across the equator at  $140^{\circ}\text{W}$ . They found that PIC residence time in the euphotic zone was 3–15 days. *Poulton et al.* [2006] also determined PIC residence times in the Atlantic as  $\sim 3$  days, hence regional studies of carbonate cycling are consistent with the global compilation data presented here.

[28] The latitudinal pattern of PIC, derived from the satellite analysis, was compared to the compilation of sediment trap carbonate fluxes [*Francois et al.*, 2002] to see how standing stock relates to carbonate rain (Figure 5). The standing stock of PIC has a systematic pattern as a

function of latitude; the higher-latitude ocean contains, on an annual average, more PIC than does the low-latitude ocean per unit area. Whereas PIC standing stocks decrease from high latitudes toward the equator, trap fluxes generally increase. The trap data, mostly within the Northern Hemisphere, show high variability but both the Atlantic and Pacific data have trends that indicate larger rain rates at low latitudes. The Pacific data show a strong gradient in trap flux between  $18^{\circ}\text{N}$  and the equator whereby carbonate rain increases by a factor of 10. The trap data indicate that carbonate rain is 5–10 times greater in the subtropical Indian Ocean compared to the Pacific, although these fluxes may be strongly influenced by monsoonal fluctuations. To minimize over generalizing the global patterns, we also compared the rain of carbonate into deep traps to PIC standing stocks in five biogeographical regions (Figure 6) [after *Longhurst*, 1998]. This analysis shows little systematic relationship between these parameters.

[29] The poor coherence between satellite PIC standing stock distributions and long-term trap data may reflect temporal variability in these data, differences in the effective sampling depth for satellites and sediment traps, or may point to processes occurring to lessen the rain of particulate carbonate in high latitudes and enhance the rain in low latitudes. One process that could impart the patterns observed would be if carbonate particles resided longer in the euphotic zone of high-latitude oceans than in low-latitude oceans. Another possibility is that PIC rain at low latitudes is dominated by particles not observed by satellites, perhaps foraminifera. Also, greater rates of water column dissolution driven by the lower saturation state at

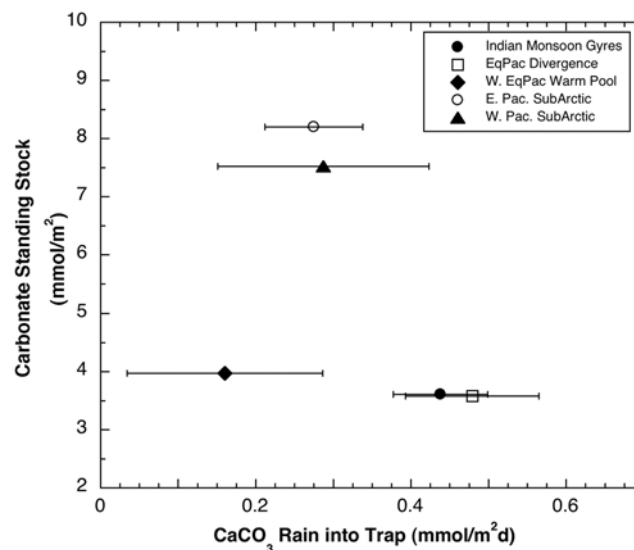


**Figure 6.** Standing stock of PIC and the PIC flux into sediment traps for five biogeochemical provinces (as defined by *Longhurst* [1998]). The PIC standing stock is the annual average value from *Balch et al.* [2005] and the trap flux is from the compilation of *Francois et al.* [2002]. The trap data include traps deployed at different locations but within the province region. The error bars represent s.d. of the mean of all the traps in a given region.



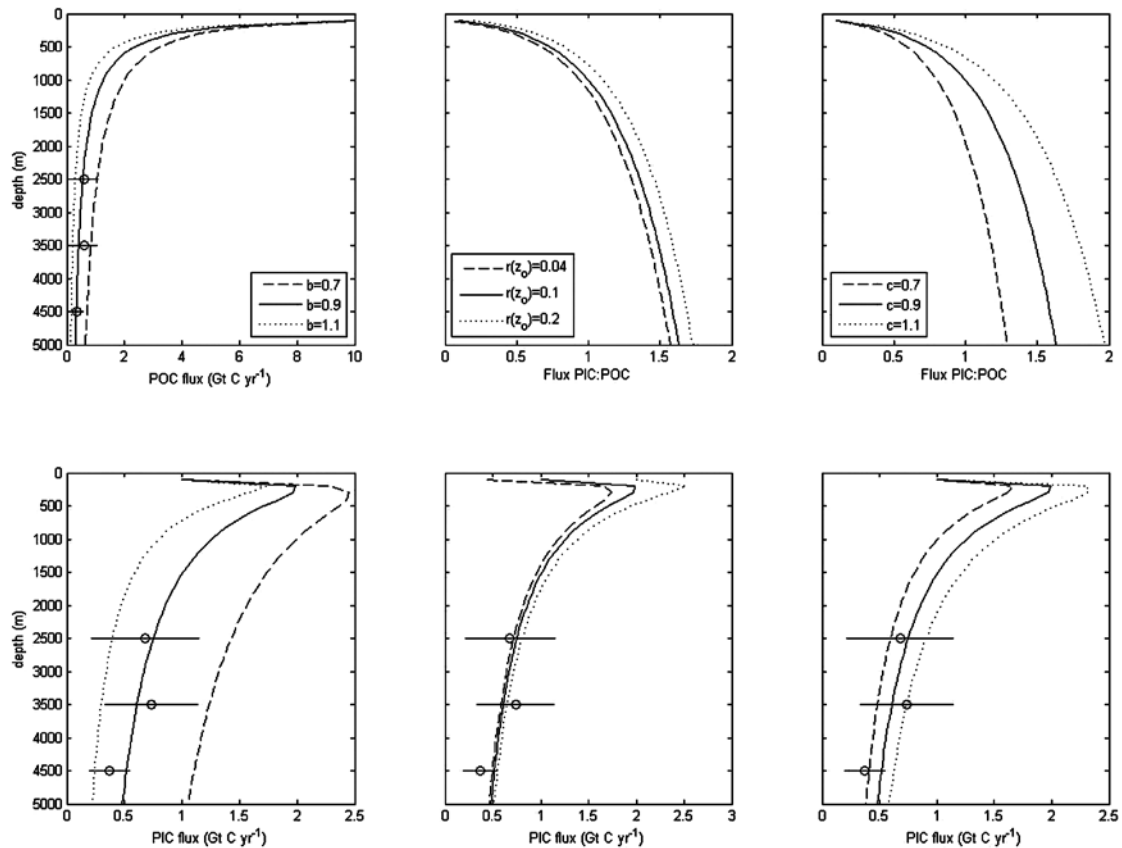


**Figure 8.** (top left) Martin function with an export value of 10 Gt C yr<sup>-1</sup> and illustrates rain versus depth for three values of *b*. The open circles are depth-binned (2000–3000, 3000–4000, 4000–5000) average sediment trap POC flux values from *Francois et al.* [2002]. (top center and right) PIC:POC versus depth patterns given different values of *r*(*z*<sub>0</sub>) and *c*. These curves use base case values *c* = 0.9, *b* = 0.9 and *r*(*z*<sub>0</sub>) = 0.1. (bottom) PIC rain predicted from the variability in the panel above. The bottom left panel demonstrates how small changes in *b* have a large impact on the predicted PIC flux. The bottom middle and right panels show much less sensitivity to PIC:POC parameterization. Measured trap PIC fluxes (open symbols, bottom panels) suggest *b* values are likely >0.9.

where  $F_{\text{POC}}$  is the sinking flux of POC,  $z$  is the depth and  $z_0$  is typically chosen to be near the base of the euphotic zone. The Martin function enjoys widespread use in 3-D models of the marine carbon cycle, which are typically evaluated with nutrient, oxygen and TCO<sub>2</sub> distributions [e.g., *Najjar et al.*, 1992; *Gnanadesikan et al.*, 2004]. *Martin et al.* [1987] chose  $b = 0.86$  as a fit to open ocean sediment trap data in the North Pacific, whereas subsequent inverse studies and model tuning exercises give values of  $b$  that vary between about 0.7 and 1.1 [*Yamanaka and Tajika*, 1996; *Schlitzer*, 2002; *Kwon and Primeau*, 2006; *Primeau*, 2006].

[32] The PIC:POC data from traps located at Sta. P, the N. Atlantic, EqPac and the W. Pacific Warm Pool (Figure 8) were each fit with an equation of the form

$$r(z) = r(z_0) + c \log[z/z_0],$$

where  $r(z)$  is the PIC:POC flux ratio,  $c$  is a slope parameter and  $r(z_0)$  is the initial export PIC:POC ratio. Fits to the four different locations provide a range in  $c$  of 0.7–1.1 and a

range in  $r(z_0)$  of 0.06–0.35. However, given reasonable bounds on PIC export (0.4–1.8 Gt PIC yr<sup>-1</sup>, this study) and POC export (8–12 Gt C yr<sup>-1</sup> [*Jin et al.*, 2007]) a reasonable range of  $r(z_0)$  parameters is 0.04–0.2. Several PIC:POC versus depth curves were generated using the equation above and the parameter ranges cited (top two right panels in Figure 8). To assess variability in POC flux, we used  $F_{\text{POC}(z_0)} = 10$  Gt POC yr<sup>-1</sup> and generated different patterns of POC versus depth by varying Martin function parameter  $b$  (top left panel in Figure 8). The product of POC flux and PIC:POC at any depth produces a model pattern of PIC rain versus depth (bottom panels in Figure 8).

[33] The models show an increase in PIC flux in the upper 300 m that can not be easily explained by natural phenomena and is likely due to the functions we choose to simulate POC and PIC:POC versus depth. However, this pattern could represent carbonate added to sediment traps in shallow waters by the action of “swimmers” or selective collection of carbonate particles. We view this portion of the plots with some skepticism, yet the remaining trend in PIC rain versus depth suggests that: (1) there might be as

**Table 3.** Summary of CaCO<sub>3</sub> Flux Estimates<sup>a</sup>

Flux Term	mmol CaCO <sub>3</sub> m <sup>-2</sup> d <sup>-1</sup>	Gt PIC yr <sup>-1</sup>
Production or calcification in the euphotic zone	0.3–1.0	0.5–1.6
Export from surface (models)	0.3–1.1	0.4–1.8
Export from surface (traps, Pacific)	0.9–3.0	1.4–4.7
Dissolution in upper 200–1500 m		
Atlantic	0.3	0.1
Pacific	0.8	0.6
Indian	1.1	0.3
Total		1.0
Export to traps below 2000 m	0.38 ± 0.24	0.6 ± 0.4
Dissolution on sea floor below 2000 m (Atlantic and Pacific)	0.24 ± 0.17	0.4 ± 0.3
Burial in Holocene sediments	0.08	0.1

<sup>a</sup>Values are for global budgets, except where noted.

much as 2 Gt PIC yr<sup>-1</sup> leaving the upper ocean, (2) there could be >1 Gt PIC yr<sup>-1</sup> dissolution during settling through the upper 1500 m, and (3) there is carbonate dissolution occurring as particles settle below 2000 m, on the order of 0.1–0.2 Gt PIC yr<sup>-1</sup>. This simplified model predicts a flux of PIC of approximately 0.7 Gt PIC yr<sup>-1</sup> falling between 2000 and 5000 m, which is consistent with trap data (Figure 8).

## 7. Developing a Revised Global Carbonate Budget

[34] An updated compilation of carbonate production [Balch *et al.*, 2007], sediment trap rain [Francois *et al.*, 2002], water column and benthic dissolution rates (this paper) help refine and constrain terms in Feely *et al.*'s [2004a] carbonate budget. Globally averaged, estimates of carbonate production range from 0.5 to 1.6 Gt PIC yr<sup>-1</sup> (0.3–1.0 mmol m<sup>-2</sup>d<sup>-1</sup>) and export estimates range from 0.4 to 1.8 Gt PIC yr<sup>-1</sup> (0.3–1.1 mmol m<sup>-2</sup>d<sup>-1</sup>). Our assessment of sediment trap data suggests that fluxes of PIC below 2000 m water depth averages 0.6 ± 0.3 Gt PIC yr<sup>-1</sup> (0.4 ± 0.2 mmol m<sup>-2</sup>d<sup>-1</sup>), sea floor dissolution for sites >2000 m averages 0.4 ± 0.3 Gt PIC yr<sup>-1</sup> (0.24 ± 0.17 mmol m<sup>-2</sup>d<sup>-1</sup>) and carbonate burial in deep marine sediments is 0.1 Gt PIC yr<sup>-1</sup> (0.08 mmol m<sup>-2</sup>d<sup>-1</sup>) (Table 3). Below 2000 m, this budget compilation shows excellent agreement between estimates of carbonate fluxes determined with completely different approaches and averaging vastly different global regions. Given that dissolution of carbonate particles as they sink between 200 and 1500 m could account for 1.0 ± 0.5 Gt PIC yr<sup>-1</sup> and assuming a trap flux value of 0.6 Gt PIC yr<sup>-1</sup>, the export flux of carbonate would be constrained at 1.6 Gt PIC yr<sup>-1</sup>. This constrains carbonate production as greater or equal to 1.6 Gt PIC yr<sup>-1</sup>. Even if the upper ocean dissolution flux is overestimated by 50%, the predicted export value would be 1.1 Gt PIC yr<sup>-1</sup>, which is larger than many model-based estimates.

[35] The global averages presented above will be continually modified as more measurements and models provide

refinement of the major flux terms. The work of Milliman *et al.* [1999] and Feely *et al.* [2004a] has opened a new window into the importance of water column processing of CaCO<sub>3</sub> particles. Both the difference between export flux and flux into traps at 2000 m and water column tracer studies implicate water column dissolution as a major term in the carbonate budget.

## 8. Summary and Conclusions

[36] Various methodologies have been applied to constrain carbonate budgets and examine the role of benthic and water column dissolution of PIC. Within the North Pacific Ocean >40°N, between 200 and 1500 m, the rate of TA\* addition to well-dated water masses suggests a dissolution rate of PIC from settling particles equal to 1.7 mmol CaCO<sub>3</sub> m<sup>-2</sup>d<sup>-1</sup> (0.07 Gt PIC yr<sup>-1</sup>). Although there is a significant flux of alkalinity from outer shelf and upper slope sediments, benthic processes contribute only 5–10% of the TA\* signal because the areal extent of these sediments is small compared to the area over which the water column signal is generated.

[37] A compilation of upper ocean TA\* and water mass ages indicates that high rates of water column PIC dissolution occurs at high latitudes in the Atlantic, Indian and Pacific Oceans. Of the 1 Gt PIC yr<sup>-1</sup> dissolving during particle sinking, 60% occurs in the Pacific and 30% in the Indian Ocean. Regions of the global ocean where the saturation horizon shoals are regions where higher rates of PIC dissolution occur. Sediment trap results from Station P and EqPac support our conclusion that water column dissolution of PIC occurs to a greater extent at high latitudes.

[38] We compiled all in situ benthic carbonate dissolution rate measurements and found an average dissolution flux of 0.24 ± 0.17 (s.d., n = 37) mmol CaCO<sub>3</sub> m<sup>-2</sup>d<sup>-1</sup> for sites between 2000 and 5000 m in the Atlantic and Pacific Oceans. The relationship between TA\* and deep-water age indicates a rate of PIC dissolution of 0.05–0.06 μmoles moles CaCO<sub>3</sub> kg<sup>-1</sup> yr<sup>-1</sup> [Feely *et al.*, 2002; Sabine *et al.*, 2002; Chung *et al.*, 2003]. Applied to a water column 1500–2000 m thick, these values translate to 0.21–0.33 mmol CaCO<sub>3</sub> m<sup>-2</sup>d<sup>-1</sup>. Benthic dissolution, therefore, can account for most of the observed changes in TA\* in deep waters if the water column in contact with the sediments is 1500–2000 m thick. The increase in TA\* near the sediment boundaries provides further support for a sedimentary source. Benthic carbonate dissolution rates are highest between 3500 and 5000 m water depth.

[39] The global average flux of carbonate particles through 2000 m is 0.38 ± 0.24 mmol m<sup>-2</sup>d<sup>-1</sup> (0.6 ± 0.4 Gt PIC yr<sup>-1</sup>) and the pattern of carbonate rain as a function of latitude shows a weak trend toward greater fluxes at low latitudes. The pattern of PIC standing stocks in the euphotic zone as determined from satellite imagery shows the opposite pattern, higher PIC at the high latitudes. The offset between the pattern of standing stock and particulate rain could imply processes controlling carbonate packaging and transport through the water column are very different at high and low latitudes. Carbonate dissolution in

undersaturated waters at high latitudes could also contribute to this offset.

[40] Most sites in the open ocean achieve PIC:POC values of  $>1$  as particles fall through 1000 m and  $>1.5$  as particles fall through 4000 m. If the rain of POC versus depth follows a Martin function, a model that predicts PIC flux from PIC:POC ratios indicates that carbonate dissolution occurs as particles settle throughout the water column, the amount of dissolution could be  $>1$  Gt PIC yr<sup>-1</sup> in the upper 1500 m, and this model confirms a flux of PIC into deep ( $>2000$  m) sediment traps of  $0.4 \text{ mmol CaCO}_3 \text{ m}^{-2} \text{ d}^{-1}$  ( $0.6 \text{ Gt PIC yr}^{-1}$ ).

[41] The global carbonate budget is far from resolved. While evidence supports the high rates of PIC dissolution in the upper water column, few models of production or export can support any dissolution given a sediment trap flux of  $0.6 \text{ Gt PIC yr}^{-1}$ . However, the measurements by Poulton *et al.* [2006] do indicate high rates of carbonate production over broad regional scales. It is possible that estimates of dissolution in the upper water column are exaggerated by uncertainties in mixing models used to establish water mass age. However, dissolution in the upper water column is supported by trap data and appears unbiased by the flux of alkalinity from outer shelf, upper slope sediments. The present data suggests that dissolution of settling particles occurs both in the upper water column and deep water column, to a greater extent in the upper water column, and to a greater extent at high latitudes.

[42] The export and remineralization rates of PIC and POC are critical components in controlling the pCO<sub>2</sub> content of the surface ocean [Sarmiento *et al.*, 2002]. The baseline values established here can be improved upon given continued measurements and modeling efforts dedicated to understanding carbon cycling.

[43] **Acknowledgments.** The authors would like to acknowledge US-JGOFS SMP and NSF for support of this research. This work was also supported by the National Oceanic and Atmospheric Administration (NOAA). We specifically acknowledge program managers Phil Taylor and Don Rice of the NSF Biological and Chemical Oceanography Programs, respectively, and Will Beaumont at USC and Kathy Tedesco and Mike Johnson of the NOAA Climate Program Office for their support. This is PMEL contribution 2980. Partial support for preparation of this paper was provided by the National Research Laboratory Program of the Korean Science and Engineering Foundation (K. L.).

## References

- Archer, D. (1996), A data-driven model of the global calcite lysocline, *Global Biogeochem. Cycles*, *10*, 511–526.
- Archer, D. E., H. Kheshgi, and E. Maier-Reimer (1998), The dynamics of fossil fuel CO<sub>2</sub> neutralization by marine CaCO<sub>3</sub>, *Global Biogeochem. Cycles*, *12*, 259–276.
- Armstrong, R. A., C. Lee, J. L. Hedges, S. Honjo, and S. G. Wakeham (2002), A new, mechanistic model for organic carbon fluxes in the ocean, based on the quantitative association of POC with ballast minerals, *Deep Sea Res., Part II*, *49*, 219–236.
- Bacastow, R., and E. Maier-Reimer (1990), Ocean-circulation model of the carbon cycle, *Clim. Dyn.*, *4*, 95–125.
- Balch, W. M., and K. A. Kilpatrick (1996), Calcification rates in the equatorial Pacific along 140°W, *Deep Sea Res., Part II*, *43*, 971–993.
- Balch, W. M., H. R. Gordon, B. C. Bowler, D. T. Drapeau, and E. S. Booth (2005), Calcium carbonate budgets in the surface global ocean based on MODIS data, *J. Geophys. Res.*, *110*, C07001, doi:10.1029/2004JC002560.
- Balch, W. M., D. T. Drapeau, B. C. Bowler, and E. Booth (2007), Prediction of pelagic calcification rates using satellite-measurements, *Deep Sea Res., Part II*, in press.
- Berelson, W. (2001), POC fluxes into the ocean interior: A comparison of 4 US-JGOFS regional studies, *Oceanography*, *14*, 59–67.
- Berelson, W. M., D. E. Hammond, and K. S. Johnson (1987), Benthic fluxes and the cycling of biogenic silica and carbon in two southern California borderland basins, *Geochim. Cosmochim. Acta*, *51*, 1345–1363.
- Berelson, W. M., D. E. Hammond, and G. Cutter (1990), In situ measurements of calcium carbonate dissolution rates in deep-sea sediments, *Geochim. Cosmochim. Acta*, *54*, 3013–3020.
- Berelson, W. M., D. E. Hammond, J. McManus, and T. E. Kilgore (1994), Dissolution kinetics of calcium carbonate in equatorial Pacific sediments, *Global Biogeochem. Cycles*, *8*, 219–235.
- Berelson, W., J. McManus, K. Coale, K. Johnson, T. Kilgore, D. Burdige, and C. Piskaln (1996), Biogenic matter diagenesis on the sea floor: A comparison between two continental margin transects, *J. Mar. Res.*, *54*, 731–762.
- Berelson, W. M., *et al.* (1997), Biogenic budgets of particle rain, benthic remineralization and sediment accumulation in the equatorial Pacific, *Deep Sea Res., Part II*, *44*, 2251–2282.
- Berelson, W. M., J. McManus, K. Coale, K. Johnson, D. Burdige, T. Kilgore, D. Colodner, F. Chavez, R. Kudela, and J. Boucher (2003), A time series of benthic flux measurements from Monterey Bay, CA, *Cont. Shelf Res.*, *23*, 457–481.
- Buesseler, K. O. (1991), Do upper ocean sediment traps provide an accurate record of particle flux?, *Nature*, *353*, 420–423.
- Caldeira, K., and M. E. Wickett (2003), Anthropogenic carbon and ocean pH, *Nature*, *425*, 365.
- Catubig, N. R., D. E. Archer, R. Francois, P. deMenocal, W. Howard, and E. F. Yu (1998), Global deep-sea burial rate of calcium carbonate during the Last Glacial Maximum, *Paleoceanography*, *13*(3), 298–310.
- Chen, C.-T. A. (2002), Shelf-vs. dissolution-generated alkalinity above the chemical lysocline, *Deep Sea Res., Part II*, *49*, 5365–5375.
- Chuck, A., T. Tyrrell, I. J. Totterdell, and P. M. Holligan (2005), The oceanic response to carbon emissions over the next century: investigation using three ocean carbon cycle models, *Tellus, Ser. B*, *57*, 70–86.
- Chung, S., K. Lee, R. A. Feely, C. L. Sabine, F. J. Millero, R. Wanninkhof, J. L. Bullister, R. M. Key, and T.-H. Peng (2003), Calcium carbonate budget in the Atlantic Ocean based on water column inorganic carbon chemistry, *Global Biogeochem. Cycles*, *17*(4), 1093, doi:10.1029/2002GB002001.
- Devol, A., and J. P. Christensen (1993), Benthic fluxes and nitrogen cycling in sediments of the continental margin of the eastern N. Pacific, *J. Mar. Res.*, *51*, 345–372.
- Dymond, J., and R. Collier (1988), Biogenic particle fluxes in the equatorial Pacific: Evidence for both high and low productivity during the 1982–1983 El Niño, *Global Biogeochem. Cycles*, *2*, 129–137.
- Fabry, V. J. (1989), Aragonite production by pteropod mollusks in the subarctic Pacific, *Deep Sea Res.*, *36*, 1735–1751.
- Feely, R. A., *et al.* (2002), In situ calcium carbonate dissolution in the Pacific Ocean, *Global Biogeochem. Cycles*, *16*(4), 1144, doi:10.1029/2002GB001866.
- Feely, R. A., C. L. Sabine, K. Lee, W. Berelson, J. Kleypass, V. J. Fabry, and F. J. Millero (2004a), Impact of anthropogenic CO<sub>2</sub> on the CaCO<sub>3</sub> system in the oceans, *Science*, *305*, 362–366.
- Feely, R. A., C. L. Sabine, R. Schlitzer, J. L. Bullister, S. Mecking, and D. Greeley (2004b), Oxygen utilization and organic carbon remineralization in the upper water column of the Pacific Ocean, *J. Oceanogr.*, *60*(1), 45–52.
- Francois, R., S. Honjo, R. Krishfield, and S. Manganini (2002), Factors controlling the flux of organic carbon to the bathypelagic zone of the ocean, *Global Biogeochem. Cycles*, *16*(4), 1087, doi:10.1029/2001GB001722.
- Friis, K., R. G. Najjar, M. J. Follows, and S. Dutkiewicz (2006), Possible overestimation of shallow-depth calcium carbonate dissolution in the ocean, *Global Biogeochem. Cycles*, *20*, GB4019, doi:10.1029/2006GB002727.
- Friis, K., R. G. Najjar, M. J. Follows, S. Dutkiewicz, A. Kortzinger, and K. M. Johnson (2007), Dissolution of calcium carbonate: Observations and model results in the North Atlantic, *Biogeosciences*, in press.
- Garçon, V. C., and J.-F. Minster (1988), Heat, carbon and water fluxes in a 12-box model of the world ocean, *Tellus, Ser. B*, *40*, 161–177.
- Gattuso, J.-P., M. Frankignoulle, I. Bourge, S. Romaine, and R. W. Buddemeier (1998), Effect of calcium carbonate saturation of seawater on coral calcification, *Global Planet. Change*, *18*, 37–46.
- Gnanadesikan, A., J. P. Dunne, R. M. Key, K. Matsumoto, J. L. Sarmiento, R. D. Slater, and P. S. Swathi (2004), Oceanic ventilation and biogeo-

- chemical cycling: Understanding the physical mechanisms that produce realistic distributions of tracers and productivity, *Global Biogeochem. Cycles*, 18, GB4010, doi:10.1029/2003GB002097.
- Grebmeier, J. M., and C. P. McRoy (1989), Pelagic-benthic coupling on the shelf of the northern Bering and Chuckchi seas. III. Benthic food supply and carbon cycling, *Mar. Ecol. Prog. Ser.*, 53, 79–81.
- Hales, B., and S. Emerson (1996), Calcite dissolution in sediments of the Ontong-Java Plateau: In situ measurements of pore water O<sub>2</sub> and pH, *Global Biogeochem. Cycles*, 10, 527–541.
- Hales, B., and S. Emerson (1997), Calcite dissolution in sediments of the Ceara Rise: In situ measurements of porewater O<sub>2</sub>, pH and CO<sub>2</sub>, *Geochim. Cosmochim. Acta*, 61, 501–514.
- Hales, B., S. Emerson, and D. Archer (1994), Respiration and dissolution in the sediments of the western North Atlantic: Estimates from models of in situ microelectrode measurements of porewater oxygen and pH, *Deep Sea Res., Part I*, 41, 695–719.
- Hammond, D. E., P. Giordani, W. M. Berelson, and R. Poletti (1999), Diagenesis of carbon and nutrients and benthic exchange in sediments of the N. Adriatic Sea, *Mar. Chem.*, 66, 53–79.
- Honjo, S., and S. Manganini (1993), Annual biogenic particle fluxes to the interior of the North Atlantic Ocean: Studies at 34°N 21°W and 48°N 21°W, *Deep Sea Res., Part II*, 40, 587–607.
- Honjo, S., J. Dymond, R. Collier, and S. J. Manganini (1995), Export production of particles to the interior of equatorial Pacific Ocean during 1992 EqPac experiment, *Deep Sea Res., Part II*, 42, 831–870.
- Jahnke, R. A. (1990), Early diagenesis and recycling of biogenic debris at the sea floor, Santa Monica Basin, California, *J. Mar. Res.*, 48, 413–436.
- Jahnke, R. A., and D. B. Jahnke (2000), Rates of C, N, P and Si recycling and denitrification at the US Mid-Atlantic continental slope depocenter, *Deep Sea Res., Part I*, 47, 1405–1428.
- Jahnke, R. A., D. B. Craven, and J.-F. Gaillard (1994), The influence of organic matter diagenesis on CaCO<sub>3</sub> dissolution at the deep-sea floor, *Geochim. Cosmochim. Acta*, 58, 2799–2809.
- Jahnke, R. A., D. B. Craven, D. C. McCorkle, and C. E. Reimers (1997), CaCO<sub>3</sub> dissolution in California continental margin sediments: The influence of organic matter remineralization, *Geochim. Cosmochim. Acta*, 61, 3587–3604.
- Jin, X., R. G. Najjar, F. Louanchi, and S. C. Doney (2007), A modeling study of the seasonal oxygen budget of the global ocean, *J. Geophys. Res.*, doi:10.1029/2006JC003731, in press.
- Kawahata, H., A. Suzuki, and H. Ohta (2000), Export fluxes in the Western Pacific Warm Pool, *Deep Sea Res., Part I*, 47, 2061–2091.
- Klaas, C., and D. E. Archer (2002), Association of sinking organic matter with various types of mineral ballast in the deep sea: Implications for the rain ratio, *Global Biogeochem. Cycles*, 16(4), 1116, doi:10.1029/2001GB001765.
- Kleypas, J. A., R. W. Buddemeier, D. Archer, J.-P. Gattuso, C. Langdon, and B. N. Opdyke (1999), Geochemical consequences of increased atmospheric carbon dioxide on coral reefs, *Science*, 284, 118–120.
- Kwon, E. Y., and F. Primeau (2006), Optimization and sensitivity study of a biogeochemistry ocean model using an implicit solver and in situ phosphate data, *Global Biogeochem. Cycles*, 20, GB4009, doi:10.1029/2005GB002631.
- Lampitt, R. S., and A. N. Antia (1997), Particle flux in deep seas: Regional characteristics and temporal variability, *Deep Sea Res., Part I*, 44, 1377–1403.
- Lampitt, R. S., B. J. Bett, K. Kiriakoulakis, E. E. Popova, O. Ragueneau, A. Vangrieshem, and G. A. Wolff (2001), Material supply to the abyssal seafloor in the Northeast Atlantic, *Prog. Oceanogr.*, 50, 27–63.
- Langdon, C., and M. J. Atkinson (2005), Effect of elevated pCO<sub>2</sub> on photosynthesis and calcification of corals and interactions with seasonal change in temperature/irradiance and nutrient enrichment, *J. Geophys. Res.*, 110, C09S07, doi:10.1029/2004JC002576.
- Langdon, C., W. S. Broecker, D. E. Hammond, E. Glenn, K. Fitzsimmons, S. G. Nelson, T.-H. Peng, I. Hadjias, and G. Bonani (2003), Effect of elevated CO<sub>2</sub> on the community metabolism of an experimental coral reef, *Global Biogeochem. Cycles*, 17(1), 1011, doi:10.1029/2002GB001941.
- Laws, E. A., P. G. Falkowski, W. O. Smith, H. Ducklow, and J. J. McCarthy (2000), Temperature effects on export production in the open ocean, *Global Biogeochem. Cycles*, 14, 1231–1246.
- Lee, K. (2001), Global net community production estimated from the annual cycle of surface water total dissolved inorganic carbon, *Limnol. Oceanogr.*, 46, 1287–1297.
- Longhurst, A. R. (1998), *Ecological Geography of the Sea*, 398 pp, Elsevier, New York.
- Martin, J. H., G. A. Knauer, D. M. Karl, and W. W. Broenkow (1987), VERTEX: Carbon cycling in the northeast Pacific, *Deep Sea Res.*, 34, 267–285.
- Martin, W. R., and F. L. Sayles (1996), CaCO<sub>3</sub> dissolution in sediments of the Ceara Rise, western equatorial Atlantic, *Geochim. Cosmochim. Acta*, 60, 243–263.
- Milliman, J. D. (1993), Production and accumulation of calcium carbonate in the ocean: Budget of a nonsteady state, *Global Biogeochem. Cycles*, 7, 927–957.
- Milliman, J. D., P. J. Troy, W. M. Balch, A. K. Adams, Y.-H. Li, and F. T. MacKenzie (1999), Biologically-mediated dissolution of calcium carbonate above the chemical lysocline?, *Deep Sea Res., Part I*, 46, 1653–1669.
- Moore, J. K., S. C. Doney, D. M. Glover, and I. Y. Fung (2002), Iron cycling and nutrient limitation patterns in surface waters of the world ocean, *Deep Sea Res., Part II*, 49, 463–508.
- Moore, J. K., S. C. Doney, and K. Lindsay (2004), Upper ocean ecosystem dynamics and iron cycling in a global three-dimensional model, *Global Biogeochem. Cycles*, 18, GB4028, doi:10.1029/2004GB002220.
- Murnane, R. J., J. L. Sarmiento, and C. Le Quéré (1999), Spatial distribution of air-sea CO<sub>2</sub> fluxes and the interhemispheric transport of carbon by the oceans, *Global Biogeochem. Cycles*, 13, 287–305.
- Najjar, R. G., J. L. Sarmiento, and J. R. Toggweiler (1992), Downward transport and fate of organic matter in the ocean: Simulations with a general circulation model, *Global Biogeochem. Cycles*, 6, 45–76.
- Orr, J. C., et al. (2005), Anthropogenic ocean acidification over the twenty-first century and its impact on calcifying organisms, *Nature*, 437, 681–686.
- Pfeifer, K., C. Hensen, M. Adler, F. Wenzhofer, B. Weber, and H. D. Schulz (2003), Modeling of subsurface calcite dissolution, including the respiration and reoxidation processes of marine sediments in the region of equatorial upwelling off Gabon, *Geochim. Cosmochim. Acta*, 66, 4247–4259.
- Poulton, A. J., R. Sanders, P. M. Holligan, M. C. Stinchcombe, T. T. Adey, L. Brown, and K. Chamberlain (2006), Phytoplankton mineralization in the tropical and subtropical Atlantic Ocean, *Global Biogeochem. Cycles*, 20, GB4002, doi:10.1029/2006GB002712.
- Primeau, F. (2006), On the variability of the exponent in the powerlaw depth dependence of POC flux estimated from sediment traps, *Deep Sea Res., Part I*, 53, 1335–1343, doi:10.1016/j.dsr.2006.06.003.
- Rabouille, C., et al. (2001), Imbalance in the carbonate budget of surficial sediments in the North Atlantic Ocean: Variations over last millennium?, *Prog. Oceanogr.*, 50, 201–221.
- Reimers, C. E., R. A. Jahnke, and D. C. McCorkle (1992), Carbon fluxes and burial rates over the continental slope and rise off central California with implications for the global carbon cycle, *Global Biogeochem. Cycles*, 6, 199–224.
- Riebesell, U., I. Zondervan, B. Rost, P. D. Tortell, R. E. Zeebe, and F. M. M. Morel (2000), Reduced calcification of marine plankton in response to increased atmospheric CO<sub>2</sub>, *Nature*, 407, 364–367.
- Rodier, M., and R. Le Borgne (1997), Export of particles at the equator in the western and central Pacific Ocean, *Deep Sea Res., Part II*, 44, 2085–2113.
- Royal Society (2005), Ocean acidification due to increasing atmospheric carbon dioxide, *Policy Doc. 12/05*, 223 pp., Royal Society, London.
- Sabine, C. L., R. M. Key, R. A. Feely, and D. Greeley (2002), Inorganic carbon in the Indian Ocean, *Global Biogeochem. Cycles*, 16(4), 1067, doi:10.1029/2002GB001869.
- Sabine, C. L., et al. (2004), The oceanic sink for anthropogenic CO<sub>2</sub>, *Science*, 305, 367–371.
- Sarmiento, J. L., J. Dunne, A. Gnanadesikan, R. M. Key, K. Matsumoto, and R. Slater (2002), A new estimate of the CaCO<sub>3</sub> to organic carbon export ratio, *Global Biogeochem. Cycles*, 16(4), 1107, doi:10.1029/2002GB001919.
- Sayles, F. L., W. R. Martin, Z. Chase, and R. F. Anderson (2001), Benthic remineralization and burial of biogenic SiO<sub>2</sub> CaCO<sub>3</sub>, organic carbon and detrital material in the Southern Ocean along a transect at 170°W, *Deep Sea Res., Part II*, 48, 4323–4383.
- Schiebel, R. (2002), Planktic foraminiferal sedimentation and the marine calcite budget, *Global Biogeochem. Cycles*, 16(4), 1065, doi:10.1029/2001GB001459.
- Schlitzer, R. (2002), Carbon export fluxes in the Southern Ocean: Results from inverse modeling and comparison with satellite based estimates, *Deep Sea Res., Part II*, 49, 1623–1644.
- Shaffer, G. (1993), Effects of the marine biota on global carbon cycling, in *The Global Carbon Cycle, NATO ASI Ser.*, vol. I15, *Global Environmental Change*, edited by M. Heimann, pp. 431–455, Springer, New York.

- Ståhl, H., A. Tengberg, J. Brunnegård, and P. O. Hall (2004), Recycling and burial of organic carbon in sediments of the Porcupine Abyssal Plain, NE Atlantic, *Deep Sea Res., Part I*, 51, 777–791.
- Tsunogai, S., and S. Noriki (1991), Particles fluxes of carbon and organic carbon in the ocean: Is the marine biological activity working as a sink of the atmospheric carbon?, *Tellus, Ser. B*, 43, 256–266.
- Wenzhofer, F., M. Adler, O. Kohls, C. Hensen, B. Strotmann, S. Boehme, and H. D. Schulz (2001), Calcite dissolution driven by benthic mineralization in the deep-sea: In situ measurements, *Geochim. Cosmochim. Acta*, 65, 2677–2690.
- Wong, C. S., F. A. Whitney, D. W. Crawford, K. Iseki, R. J. Matear, W. K. Johnson, J. S. Page, and D. Timothy (1999), Seasonal and interannual variability in particle fluxes of carbon, nitrogen and silicon from times series of sediment traps at Ocean Station P, 1982–1983: Relationship to changes in subarctic primary productivity, *Deep Sea Res., Part II*, 46, 2735–2760.
- Yamanaka, Y., and E. Tajika (1996), The role of the vertical fluxes of particulate organic matter and calcite in the ocean carbon cycle: Studies using an ocean biogeochemical model, *Global Biogeochem. Cycles*, 10, 361–382.
- Yu, E.-F., R. Francois, M. P. Bacon, S. Honjo, A. P. Fleer, S. J. Manganini, L. M. M. van der Rutgers, and V. Ittekkot (2001), Trapping efficiency of bottom-tethered sediment traps estimated from the intercepted fluxes of  $^{230}\text{Th}$  and  $^{231}\text{Pa}$ , *Deep Sea Res., Part I*, 48, 865–889.
- Zondervan, I., R. E. Zeebe, B. Rost, and U. Riebesell (2001), Decreasing marine biogenic calcification: A negative feedback on rising atmospheric  $p\text{CO}_2$ , *Global Biogeochem. Cycles*, 15, 507–516.
- 
- W. M. Balch, Bigelow Laboratory for Ocean Sciences, W. Boothbay Harbor, ME 04575, USA.
- W. M. Berelson, Earth Sciences Department, University of Southern California, 3651 University Avenue, Los Angeles, CA 90089-0740, USA. (berelson@earth.usc.edu)
- R. A. Feely and C. Sabine, Pacific Marine Environmental Laboratory, NOAA, Seattle, WA 98115, USA.
- K. Lee, Pohang University of Science and Technology, Pohang, South Korea.
- R. Najjar, Penn State University, University Park, PA 16802-5013, USA.